THE JOURNAL OF BIOLOGICAL CHEMISTRY
Vol. 278, No. 42, Issue of October 17, pp. 41302–41308, 2003

Printed in U.S.A.

The Phosphonopyruvate Decarboxylase from *Bacteroides fragilis**

Received for publication, June 6, 2003, and in revised form, August 5, 2003
Published, JBC Papers in Press, August 6, 2003, DOI 10.1074/jbc.M305976200

Guofeng Zhang, Jiaying Dai, Zhibing Lu, and Debra Dunaway-Mariano‡

From the Department of Chemistry, University of New Mexico, Albuquerque, New Mexico 87131-0001

The *Bacteroides fragilis* capsular polysaccharide complex is the major virulence factor for abscess formation in human hosts. Polysaccharide B of this complex contains a 2-aminoethylphosphonate functional group. This functional group is synthesized in three steps, one of which is catalyzed by phosphonopyruvate decarboxylase. In this paper, we report the cloning and overexpression of the *B. fragilis* phosphonopyruvate decarboxylase gene (*aepY*), purification of the phosphonopyruvate decarboxylase recombinant protein, and the extensive characterization of the reaction that it catalyzes. The homotrimeric (41,184-Da subunit) phosphonopyruvate decarboxylase catalyzes (k_{cat} = 10.2 ± 0.3 s^{-1}) the decarboxylation of phosphonopyruvate (K_m = 3.2 ± 0.2 μM) to phosphonoacetaldehyde (K_i = 15 ± 2 μM) and carbon dioxide at an optimal pH range of 7.0–7.5. Thiamine pyrophosphate (K_m = 13 ± 2 μM) and certain divalent metal ions (Mg(II) K_m = 82 ± 8 μM; Mn(II) K_m = 13 ± 1 μM; Ca(II) K_m = 78 ± 6 μM) serve as cofactors. Phosphonopyruvate decarboxylase is a member of the α-ketodecarboxylase family that includes sulfopyruvate decarboxylase, acetohydroxy acid synthase/acetolactate synthase, benzoylformate decarboxylase, glyoxylate carboligase, indole pyruvate decarboxylase, pyruvate decarboxylase, the acetyl phosphate-producing pyruvate oxidase, and the acetate-producing pyruvate oxidase. The Mg(II) binding residue Asp-260, which is located within the thiamine pyrophosphate binding motif of the α-ketodecarboxylase family, was shown by site-directed mutagenesis to play an important role in catalysis. Pyruvate (k_{cat} = 0.05 s^{-1}, K_m = 25 mM) and sulfopyruvate (k_{cat} ~ 0.05 s^{-1}; K_i = 200 ± 20 μM) are slow substrates for the phosphonopyruvate decarboxylase, indicating that this enzyme is promiscuous.

Bacteroides fragilis is a human pathogen that causes intra-abdominal abscess formation in its host (1, 2). The bacterial capsular polysaccharide complex is the major virulence factor for abscess formation. The capsular polysaccharide complex is composed of three distinct polysaccharides, polysaccharides A, B, and C (3–6). These polysaccharides consist of repeating units that contain a zwitterionic motif of negative and positive charged groups. The zwitterionic charge motif plays an essential role in the induction of the host defense response, which leads to abscess formation. The 2-aminoethylphosphonate (AEP)[1] unit of polysaccharide B contributes the positive and negative charges that form the zwitterionic motif (see Fig. 1).

AEP is the phosphonate counterpart to phosphoethanol amine, a common lipid polar head-group. The P-C bond of AEP is resistant to both chemical and enzymatic hydrolysis. The AEP unit is found in proteins (7), lipids (8, 9–12), and polysaccharides (4) located at the cell surfaces in certain parasitic organisms. These AEP conjugates either participate in host infection, as in the case of the *B. fragilis* polysaccharide B, or they are responsible for the persistence of the parasite within the host.

The presence of AEP in the *B. fragilis* polysaccharide B was first demonstrated by NMR structural analysis (3). More recently, the polysaccharide B biosynthetic pathway gene locus was sequenced (13). Three genes, *aepX*, *aepY*, and *aepZ*, which encode proteins that share significant sequence identity with the three enzymes of the AEP biosynthetic pathway, are included within this locus (Fig. 2). To our knowledge, this is the first known example of the AEP biosynthetic pathway gene cluster in a bacterium. Moreover, the opportunity now exists for the isolation of the three pathway enzymes for mechanistic study and inhibitor design. Because the AEP pathway enzymes are not present in humans, they are excellent candidates for drug targeting.

What is presently known about the AEP biosynthetic pathway and the three enzymes that catalyze it has resulted from a "patch-work" effort. The AEP biosynthetic pathway was first discovered in *Tetrahymena pyriformis* (14–17). In this organism, AEP is incorporated into phosphonolipids, which form the plasma membrane. The AEP pathway was shown to consist of the three steps depicted in Fig. 3. In the first step of the reaction, P-enolpyruvate is converted to phosphonopyruvate (Ppyr). P-enolpyruvate mutase, the enzyme that catalyzes this step, has been isolated from several different organisms and characterized (18–20). The conversion of P-enolpyruvate to Ppyr is thermodynamically unfavorable ($K_{eq} \sim 1 \times 10^{-3}$), and thus, the ensuing decarboxylation step catalyzed by Ppyr decarboxylase is required to drive the Ppyr-forming reaction forward. The *T. pyriformis* Ppyr decarboxylase is membrane-bound and difficult to isolate for characterization (21). What we do know about this enzyme derives from the study of the bacterial enzyme which functions in biosynthetic pathways leading to bialaphos, fosfomycin, and phosphinothricin tripeptide in *Streptomyces hygroscopicus* (22), *Streptomyces wendmorensis* (23, 24), and *Streptomyces viridomogenes* (25), respectively. In these pathways, P-enolpyruvate mutase and Ppyr decarboxylase collaborate to form the common precursor phosphonoacetaldehyde (Pald). The *S. hygroscopi*s Ppyr decarboxylase has been isolated and its native size and its cofactor requirement (*viz*. thiamine pyrophosphate and Mg(II)) have been defined (26).

* This work was supported by National Institutes of Health Grants GM 28688 and GM 61099. The costs of publication of this article were defrayed in part by the payment of page charges. This article must therefore be hereby marked "*advertisement*" in accordance with 18 U.S.C. Section 1734 solely to indicate this fact.

‡ To whom corresponding should be addressed. Tel.: 505-277-3776; Fax: 505-277-6202; E-mail: dd39@unm.edu.

[1] The abbreviations used are: AEP, 2-aminoethylphosphonate; P-enolpyruvate, phosphoenolpyruvate; Ppyr, phosphonopyruvate; TPP, thiamine pyrophosphate; TAPS, *N*-tris(hydroxymethyl)methyl-3-aminopropanesulfonic acid; Pald, phosphonoacetaldehyde; MES, 4-morpholineethanesulfonic acid.

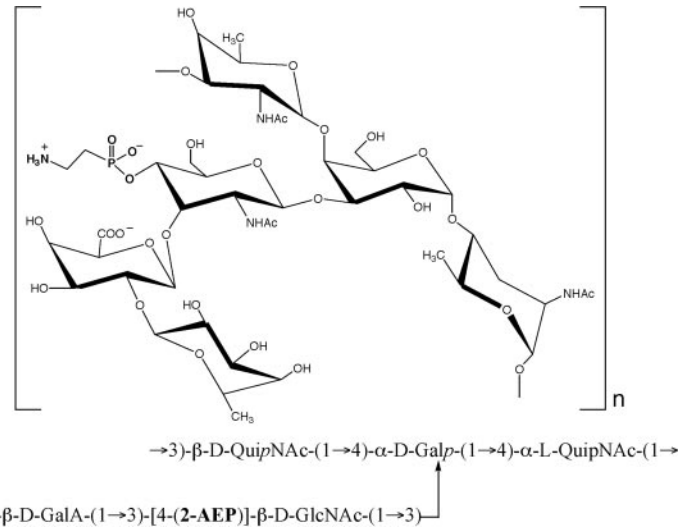

FIG. 1. **The structure of the *B. fragilis* bacterial capsular polysaccharide, polysaccharide B (4).**

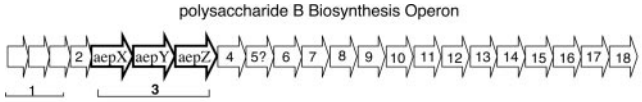

1. transcritional regulation proteins (3 genes)
2. putative glucose 1-phosphate cytidyltransferase
3. AEP biosynthetic proteins (3 genes)
   aepX: phosphoenolpyruvate mutase
   aepY: phosphonopyruvate decarboxylase
   aepZ: 2-aminoethylphosphonate aminotransferase
4. putative flippase
5. unknown function
6. putative α-1,2-fucosyltransferase
7. putative nucleotide sugar epimerase
8. putative UDP-glucose dehydrogenase
9. putative glycosyltransferase
10. putative glycosyltransferase
11. putative repeat unit polymerase
12. putative glycosyltransferase
13. putative epimerase/dehydratase
14. 3,5-epimerase
15. dTDP-4-keto-rhamnose reductase
16. putative glucosyltransferase
17. putative epimerase/dehydratase
18. putative UndP-GlcNAc-phosphotransferase

FIG. 2. **The *B. fragilis* polysaccharide B biosynthetic pathway gene locus (13).** The three AEP biosynthetic pathway genes are: *aepX* (P-enolpyruvate mutase), *aepY* (Ppyr decarboxylase), and *aepZ* (Pald transaminase). The *arrows* designate the transcription direction for each open reading frame.

As with the Ppyr decarboxylase of *Tetrahymena pyriformis*, the third enzyme of the pathway, Pald transaminase proved to be membrane-bound and difficult to isolate. Using partially purified enzyme, Kim (21) was able to demonstrate catalysis of pyridoxal phosphate-dependent transamination of Pald with L-alanine functioning as the ammonium group donor. A related transaminase can be found in bacteria adapted for the use of AEP as an alternate source of carbon, nitrogen, and phosphorous. Because the physiological reaction is catalyzed in the direction of Pald formation, this enzyme has become known as AEP transaminase (27–31). It, too, is dependent on pyridoxal phosphate; however, the ammonium group acceptor is not pyruvate but rather L-glutamate (32). Nevertheless, the bacterial AEP transaminase shares sufficient sequence identity with the *B. fragilis* Pald transaminase to indicate that the two enzymes share common ancestry.

The AEP pathway enzymes of *B. fragilis* have not been isolated for characterization. Our goal was to express the *B. fragilis* AEP pathway genes in *Escherichia coli* for purification and study of the three pathway enzymes. In this paper, we report the cloning and overexpression of the *B. fragilis* Ppyr decarboxylase gene (*aepY*), purification of the protein, and for the first time, an in-depth study of the Ppyr decarboxylase.

EXPERIMENTAL PROCEDURES

Materials—Thiamine pyrophosphate chloride (TPP), dihydro-β-nicotinamide adenine dinucleotide (β-NADH), yeast alcohol dehydrogenase, and the buffers used in protein purification and kinetic assays were purchased from Sigma and used without further purification. Phosphonopyruvate and sulfopyruvate were synthesized according to the published methods (33, 34). Recombinant *Bacillus cereus* phosphonoacetaldehyde hydrolase was purified as described previously (35). *B. fragilis* genomic DNA was purchased from American Type Culture Collection (ATCC 25285D). The primers used in PCR-based DNA amplification were custom synthesized at Invitrogen. For the cloning of the phosphonopyruvate decarboxylase gene, the sequence of the 5′ to 3′ primer was ATTCAGACGCATATGGTAAGTGTA and that of the 3′ to 5′ primer was TCTTTCTTTGGATCCTCATGAATGCGT, with the introduced restriction sites underlined. The enzymes used in DNA manipulation were purchased from Invitrogen and used with the buffers provided.

PCR-based Cloning of Phosphonopyruvate Decarboxylase Gene—The genomic DNA template was denatured (30 min at 94 °C) before adding *Pfu* DNA polymerase. The target gene was amplified by 20 cycles of 94 °C denaturation for 1 min, 55 °C annealing for 50 s, and 73 °C elongation for 3.5 min. The PCR product was purified by electrophoresis and digested using *Nde*I and *Bam*HI restriction enzymes. The digest was ligated to an *Nde*I- and *Bam*HI-cut pET 3a vector. The resulting clone, named bf-Pyrdecarb-pET 3a, was used to transform *E. coli* BL21(DE3) competent cells. The gene sequence was verified by DNA sequencing carried at the Center for Genetics in Medicine, University of New Mexico School of Medicine, Albuquerque, NM.

Protein Purification—E. coli BL21(DE3) cells, transformed with the named bf-Pyrcarb-pET 3a clone, were grown to 1 $A_{600\ nm}$ at 22 °C in 1.2 liters × 4-LB media containing 100 μg/ml ampicillin. Following an 8-h induction period with 0.2 mM isopropyl-β-D-thiogalactopyranoside, the cells were harvested by centrifugation at 6500 rpm, 4 °C (all purification steps were carried out at 4 °C except where noted). The cell pellet was suspended in 100 ml of 50 mM K^+HEPES containing 5 mM $MgCl_2$ and 1 mM dithiothreitol, pH 7.5 (referred to as buffer A, hereafter). Cells were lysed at 1000 p.s.i. in a French pressure cell and then centrifuged at 20,000 rpm for 30 min. The supernatant was subjected to ammonium sulfate precipitation. The 40–85% fraction was collected by centrifugation and dissolved in buffer A for overnight dialysis against buffer A. The dialysate was chromatographed on a DEAE-Sepharose column (3.0 × 60 cm) (equilibrated with buffer A) using a 1.4-liter linear gradient of KCl (0.15–0.60 M) in buffer A as eluant. The Ppyr decarboxylase-containing fractions (eluted at ~0.35–0.40 M KCl) were identified using the spectrophotometric activity assay (described in the following section) and analyzed by SDS-PAGE. The desired Ppyr decarboxylase-containing fractions were combined and chromatographed on a hydroxylapatite column (3.0 × 40 cm) equilibrated with buffer A, using a 1.4-liter linear gradient of phosphate (0–0.25 M) in buffer A as eluant. Column fractions containing the Ppyr decarboxylase (eluted at ~0.08–0.12 M phosphate) in >95% purity (as judged by SDS-PAGE analysis) were combined and concentrated in 50 mM K^+HEPES buffer containing 5 mM $MgCl_2$, 1 mM $MnCl_2$, and 1 mM dithiothreitol, pH 7.5 (buffer B) for storage at −80 °C. Yield: 3.7 mg/g wet cell (or 22 mg of cell culture/liter).

Site-directed Mutants—The site-directed mutants E213A, D258A, and D260A were prepared by PCR and commercial primers using the clone bf-Pyrdecarb-pET 3a as a template. The PCR product was purified by electrophoresis and digested using *Nde*I and *Bam*HI restriction enzymes. The digest was ligated to an *Nde*I- and *Bam*HI-cut pET 3a vector and then used to transform competent *E. coli* BL21(DE3) cells. The gene sequence was verified by DNA sequencing carried out at the

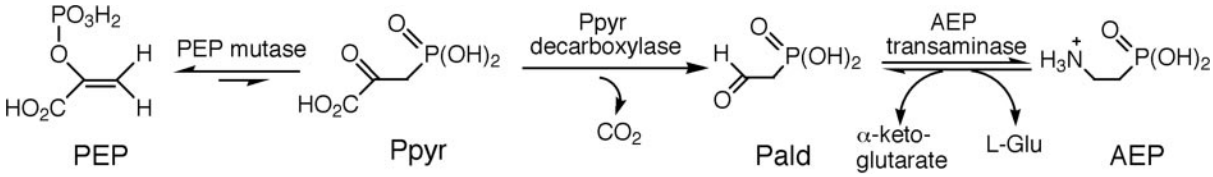

FIG. 3. **The AEP biosynthetic pathway in *T. pyriformis*.**

Center for Genetics in Medicine, University of New Mexico School of Medicine. The mutant proteins were prepared in the same manner as the wild-type Ppyr decarboxylase. The yield of the homogenous mutant proteins (as judged by SDS-PAGE analysis) are: 4 mg/g wet cell (or 20 mg of cell culture/liter) E213A, 5 mg/g wet cell (or 25 mg of cell culture/liter) D258A, and 3.5 mg/g wet cell (or 16 mg of cell culture/liter) D260A.

Ppyr Decarboxylase Molecular Size Determination—The molecular mass was calculated from the amino acid composition, derived from the gene sequence, by using the EXPASY Molecular Biology Server program Compute pI/MW (36). The molecular mass was measured by mass spectrometry (Biopolymer Mass Spectrometry Core Facility, Weill Medical College of Cornell University) and by SDS-PAGE (4% stacking gel and 12% separating gel). Commercial protein molecular weight standards were used to generate a plot of log M_r *versus* distance traveled on the gel. The size of native Ppyr decarboxylase was estimated by gel filtration column chromatography (1.6 × 60 cm, Amersham Biosciences Biotech Superdex 200-column, eluted at 4 °C with 25 mM K^+HEPES, 0.15 M KCl, pH 7.5). Commercial protein molecular weight standards were used to generate a plot of log M_r *versus* elution volume from the column.

Metal Ion Activation—The metal ion-free protein (3 mg/ml) was prepared by exhaustive dialysis against 50 mM K^+HEPES (pH 7.5, 4 °C) containing 1 mM dithiothreitol and 20 mM EDTA. The dialyzed protein was then concentrated to 10 mg/ml for kinetic study. The 1-ml reaction mixture contained 50 mM K^+HEPES (pH 7.3, 25 °C), 50 μM Ppyr, 0.15 mM NADH, 1.5 mM TPP, 1 μM wild-type phosphonoacetaldehyde hydrolase, 10 units of alcohol dehydrogenase, 0.02 μM metal-free Ppyr decarboxylase, and various concentrations of metal ions. The reactions were monitored at 340 nm ($\Delta\epsilon$ = 6,200 M^{-1} cm^{-1}). The initial velocity data were fitted to Equation 1 to obtain the dissociation constant (K_m) for the enzyme-metal ion complex,

$$V_0 = V_{max}[S]/(K_m+[S]) \quad \text{(Eq. 1)}$$

where [S] is the metal ion concentration, V_0 is the initial velocity, V_{max} is the maximum velocity, and K_m is the Michaelis-Menten constant (or in this case the K_d).

Thiamine Pyrophosphate Activation—The 1-ml reaction mixture contained 50 mM K^+HEPES (pH 7.3, 25 °C), 50 μM Ppyr, 0.15 mM NADH, 5 mM $MgCl_2$, 1 mM $MnCl_2$, 1 μM wild-type phosphonoacetaldehyde hydrolase, 10 units of alcohol dehydrogenase, 0.02 μM of dialyzed Ppyr decarboxylase (prepared as described above), and various concentrations of TPP. The reactions were monitored at 340 nm ($\Delta\epsilon$ = 6,200 M^{-1} cm^{-1}). The initial velocity data were fitted to Equation 1 to obtain the dissociation constant for the TPP-enzyme complex.

Steady-state Kinetic Constant Determination—The K_m and k_{cat} values for wild-type and mutant Ppyr decarboxylase catalysis were determined from the initial velocity data measured as a function of phosphonopyruvate concentration. The 1 ml of reaction solution contained varying concentrations of phosphonopyruvate (0.5–10 K_m), 5 mM $MgCl_2$, 1 mM $MnCl_2$, 0.15 mM NADH, 1.5 mM TPP, 1 μM wild-type phosphonoacetaldehyde hydrolase, and 10 units of alcohol dehydrogenase in 50 mM K^+HEPES (pH 7.3, 25 °C). Reactions were monitored at 340 nm. The initial velocity data were analyzed using Equation 1, wherein [S] is the phosphonopyruvate concentration. The k_{cat} was calculated from V_{max} and the enzyme concentration using the equation $k_{cat} = V_{max}/[E]$. The enzyme concentration was determined using the Bradford method (37).

pH-Rate Profile Determination—The initial velocity data were measured as a function of the reaction pH by using the following buffers at the indicated pH values: 50 mM MES (pH 6.0–6.8), 50 mM HEPES (pH 6.8–8.0), and 50 mM TAPS (pH 8.0–8.7). Each buffer solution contained 5 mM $MgCl_2$ and 1 mM $MnCl_2$ at a total chloride concentration of 75 mM (adjusted with 2 M KCl). At pH values where the reaction buffers were switched, the kinetic measurement was made with each of the two buffers to test for a possible buffer effect on the reaction rate. The k_{cat} and k_{cat}/K_m values were determined as described in the previous section and fitted to Equation 2 using the computer program KaleidaGraph,

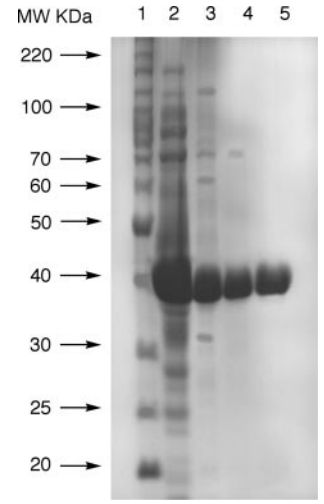

FIG. 4. **Coomassie Blue-stained SDS-PAGE of the *B. fragilis* Ppyr decarboxylase isolated at each stage of the purification procedure.** *Lane 1*, protein standards; *lane 2*, total soluble protein; *lane 3*, the protein fraction precipitated between 40–85% ammonium sulfate at 0 °C; *lane 4*, combined Ppyr decarboxylase fraction after DEAE-Sepharose column; *lane 5*, combined Ppyr decarboxylase fraction after hydroxylapatite column.

$$\log Y = \log(C/(1+[H]/K_a + K_b/[H])) \quad \text{(Eq. 2)}$$

where Y is k_{cat} or k_{cat}/K_m, [H] is the hydrogen ion concentration, C is the k_{cat} or k_{cat}/K_m value where it does not change with pH. K_a is the acid dissociation constant, and K_b is the base dissociation constant.

Screening of Alternative Substrates and Inhibitors—Substrate activity was observed with pyruvate and sulfopyruvate. The pyruvate reaction was monitored at 340 nm ($\Delta\epsilon$ = 6,200 M^{-1} cm^{-1}) by using the alcohol dehydrogenase/NADH coupling system. The 1 ml of reaction mixture contained 50 mM K^+HEPES (pH 7.3, 25 °C), 5 mM $MgCl_2$, 1 mM $MnCl_2$, 0.15 mM NADH, 1.5 mM TPP, 1.8 μM Ppyr decarboxylase, 10 units of alcohol dehydrogenase, and various concentrations of pyruvate (3–50 mM). The initial velocity data were analyzed using Equation 1.

The sulfopyruvate reaction was monitored by ^{1}H NMR. Sulfopyruvate (1 mM) was incubated for 1.5 h in 1 ml of D_2O containing 0.5 μM Ppyr decarboxylase, 1 mM $MgCl_2$, 0.4 mM TPP, and 10 mM K^+HEPES (pD 7.6, 25 °C) before recording the NMR spectrum. ^{1}H NMR spectra were measured with a Bruker Advance 500-MHz NMR spectrometer using D_2O as the solvent and at a probe temperature of 24–26 °C. The chemical shift data are reported with respect to the external reference (trimethysilyl)-propanesulfonic acid for ^{1}H NMR. Control reactions were carried out under the same conditions, except that Ppyr decarboxylase was omitted.

Pald Inhibition of Ppyr Decarboxylase Catalyzed Decarboxylation of Pyruvate—The 1-ml reaction mixtures contained 50 mM K^+HEPES, 5 mM $MgCl_2$, 1 mM $MnCl_2$, 10 mM pyruvate, 10 units of alcohol dehydrogenase, 0.15 mM NADH, 1.5 mM TPP, 1.8 μM decarboxylase, and various concentrations of Pald (0–300 μM). Initial velocities were measured at 340 nm and analyzed using Dixon Equation 3 for a competitive inhibition pattern,

$$\frac{1}{v} = \frac{K_m}{V_{max}[S]K_i}[I] + \frac{1}{V_{max}\left(1+\frac{K_m}{[S]}\right)} \quad \text{(Eq. 3)}$$

where v is the initial velocity, V_{max} is the maximum velocity, [S] is the substrate concentration (here it is 10 mM pyruvate), K_m is the Michaelis-Menten constant of pyruvate, [I] is the inhibitor concentration and K_i is the inhibition constant.

TABLE I
Experimental protocal for purification of B. fragilis Ppyr decarboxylase from E. coli BL21 (DE3) cells, transformed with the bf-Pyrcarb-pET 3a clone

Purification steps	Total protein	Total activity	Specific activity	Activity recovery	Purification
	g	*units*[a]	*units/mg*	%	*activity-fold*
Extract from 30 g of wet cells	10	6200	0.62	100	
Ammonium sulfate (40-85%)	2	3500	1.8	60	3
DEAE-Sepharose	0.20	2200	10.5	35	17
Hydroxylapatite	0.11	1344	12.1	20	20

[a] One activity unit is defined as the amount of enzyme required to produce 1 μmol of Pald/min in 50 mM K^+HEPES, pH 7.3, 5 mM $MgCl_2$ and 1.5 mM TPP at 25 °C.

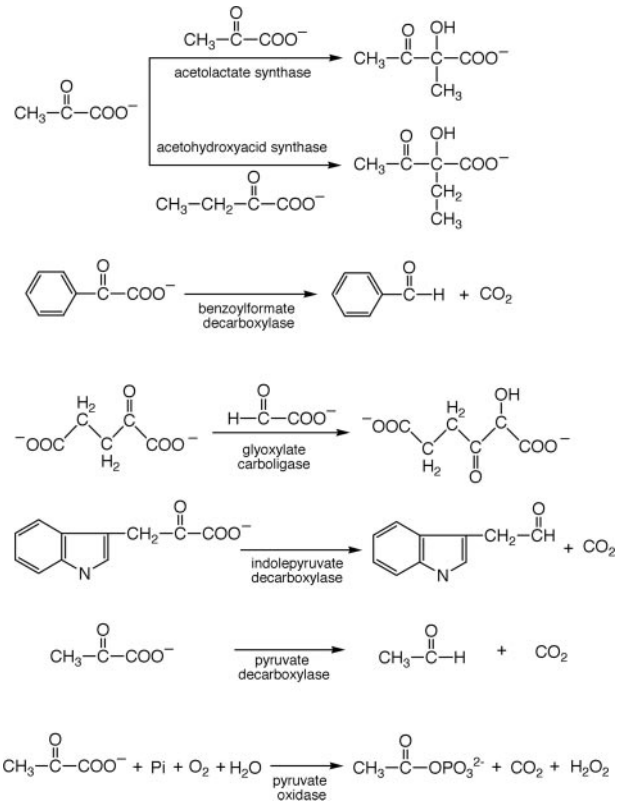

FIG. 5. **The decarboxylation reactions of the α-keto carboxylate substrates for the Ppyr decarboxylase-containing enzyme family.**

TABLE II
Metal ion dependence of steady-state kinetic constants

The metal ion dependence of the steady-state kinetic constants for Ppyr decarboxylase catalysis was measured in the presence of saturating phosphonopyruvate (50 μM) and TPP (1.5 mM) at pH 7.3 and 25 °C. Co(II), Ni(II), and Zn(II) were not activators.

Metal activator	Activator K_m	k_{cat}
	μM	s^{-1}
Mg(II)	82 ± 8	8.7 ± 0.2
Mn(II)	13 ± 1	10.2 ± 0.3
Ca(II)	78 ± 6	9.3 ± 0.2

RESULTS AND DISCUSSION

Protein Purification and Size Determination—The DNA sequence of the cloned gene agreed with the published sequence (GenBank™ accession number AF285774_6). The recombinant Ppyr decarboxylase was purified to homogeneity (see Fig. 4) by using the 4-step protocol summarized in Table I in an overall yield of 3.7 mg/g wet cells. The steady-state kinetic constants for catalyzed decarboxylation of phosphonopyruvate are: $k_{cat} = 10.2 \pm 0.3\ s^{-1}$; $K_m = 3.2 \pm 0.2\ \mu M$; and $k_{cat}/K_m = 3.2 \times 10^6\ s^{-1}\ M^{-1}$, as determined at 25 °C under optimal reaction conditions (*viz*. pH 7.3, 5 mM $MgCl_2$, 1 mM $MnCl_2$, 200 μM TPP).

The theoretical molecular weight of the phosphonopyruvate decarboxylase calculated from the amino acid sequence was 41,184, which agrees with the experimental molecular weight of 41,199, measured by matrix-assisted laser desorption ionization time-of-flight mass spectrometry. The subunit size estimated by SDS-PAGE analysis was 40 kDa compared with the native protein size of 120 kDa determined by gel filtration chromatography. Thus, the quaternary structure of Ppyr decarboxylase appears to be homotrimeric. (The *S. hygroscopicus* native Ppyr decarboxylase molecular size was reported as 135 kDa (26)).

Sequence Homologs—At the time of this writing, there are a total of seven Ppyr decarboxylase sequences listed in the Protein Data Bank. The Ppyr decarboxylase-encoding genes in *B. fragilis* (NCBI protein data bank ID code AAG26466) (378 amino acids), *Bacteroides thetaiotaomicron* (NCBI protein data bank ID code NP_810632) (374 amino acids), *Amycolatopsis orientalis* (NCBI protein data bank ID code CAB45023) (371 amino acids), and *Clostridium tetani E88* (NCBI protein data bank ID code NP_782297) (376 amino acids) are positioned between the genes encoding homologs of P-enolpyruvate mutase and AEP transaminase. Pairwise sequence alignments made with the *B. fragilis* Ppyr decarboxylase (which activity has been demonstrated in this work) demonstrated 76, 35, and 43% sequence identity, respectively. The other three Ppyr decarboxylases (401, 384, and 397 amino acids long, respectively) function in the bialaphos, fosfomycin, and phosphinothricin tripeptide biosynthetic pathways of *S. hygroscopicus* (22), *S. wendmorensis* (23, 24) and *S. viridomogenes* (25), respectively. A pairwise sequence alignment of these three Ppyr decarboxylases with the Ppyr decarboxylase from *B. fragilis* identified 34, 50, and 32% sequence identities, respectively.

A ClustalW-based sequence alignment of the seven Ppyr decarboxylase sequences identified 61 stringently conserved residues (16%). A total of 26 of the 61 stringently conserved residues are polar and, thus, are potential candidates for catalytic residues and for substrate- or cofactor-binding residues.

The *B. fragilis* Ppyr decarboxylase sequence was used as the query in a BLAST (Basic Local Alignment Search Tool) search of the gene data bank for protein homologs. The sulfopyruvate decarboxylase of the coenzyme M pathway, found in methane-forming bacteria (38), was identified as the closest homolog. Studies of the sulfopyruvate decarboxylase from *Methanococcus jannaschii* (39) have shown that the native enzyme is a dodecamer of 6 α-subunits (ComD 169 amino acids long; 34% sequence identity with the N-terminal half of the Ppyr decarboxylase) and 6 β-subunits (ComE 169 amino acids long; 39% sequence identity with the C-terminal half of Ppyr decarboxylase). It may be inferred that the α- and β-subunits of the sulfopyruvate decarboxylase correspond to N-terminal and C-terminal domains of the Ppyr decarboxylase.

Sulfopyruvate decarboxylase (39) and Ppyr decarboxylase are more distant members of a family of TPP- and Mg(II)-dependent decarboxylases that includes acetohydroxy acid synthase/acetolactate synthase (40), benzoylformate decar-

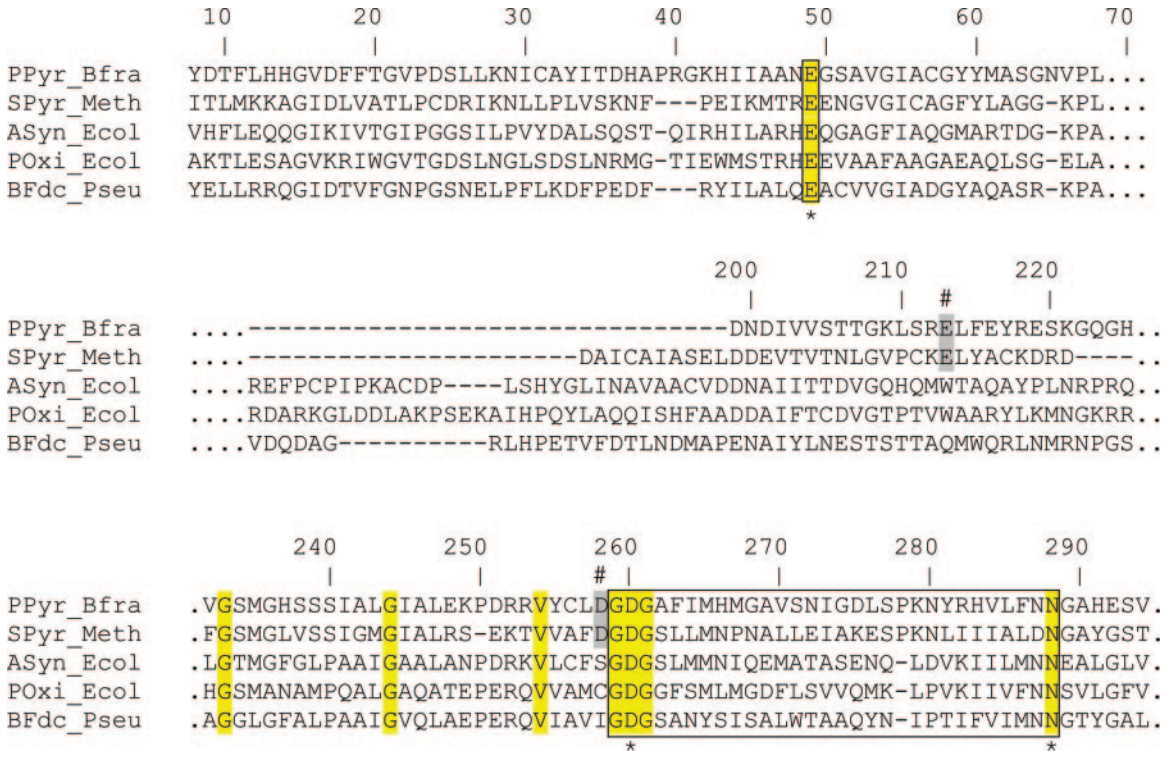

FIG. 6. **The ClustalW sequence alignment representing the Ppyr decarboxylase-containing enzyme family.** The individual sequences shown were picked as representatives of the subfamilies. The stringently conserved residues across all the subfamilies are highlighted in *yellow*, and the TPP signature motif is *boxed*. The polar residues interacting directly with Mg(II) or TPP are indicated by *, and the polar residues conserved across Ppyr decarboxylases and sulfopyruvate decarboxylases are highlighted in *gray* and marked by #. The residues are numbered for the *B. fragilis* Ppyr decarboxylase. *PPyr_Bfra*, *B. fragilis* Ppyr decarboxylase (NCBI protein data bank ID code AAG26466); *SPyr_Meth*, sulfopyruvate decarboxylase from *Methanosarcina acetivorans str. C2A* (NCBI protein data bank ID code NP_618188); *Asyn_Ecol*, the acetolactate synthase isozyme I large subunit from *E. coli CFT073* (NCBI protein data bank ID code NP_756456); *POxi_Ecol*, pyruvate oxidase from *E. coli O157* (NCBI protein data bank ID code NP_286643); *BFdc_Pseu*, benzoylformate decarboxylase from *Pseudomonas putida* (NCBI protein data bank ID code P20906).

TABLE III
Steady-state kinetic constants of wild type and mutant Ppyr

The steady-state kinetic constants of wild type and mutant Ppyr decarboxylase catalyzed decarboxylation of phosphonopyruvate (Ppyr) in the presence of 1.5 mM TPP and 5 mM $MgCl_2$ and 1 mM $MnCl_2$, at pH 7.3 and 25 °C.

Enzyme	k_{cat}	Ppyr K_m	k_{cat}/K_m
	s^{-1}	μM	$s^{-1}\cdot M^{-1}$
Wild type	10.2 ± 0.3	3.2 ± 0.2	3.2×10^6
E213A	0.48 ± 0.01	2.6 ± 0.3	1.8×10^5
D258A	0.96 ± 0.01	2100 ± 50	4.6×10^2
D260A	0.010 ± 0.001	17.1 ± 0.8	5.8×10^2

boxylase (41), glyoxylate carboligase, indole pyruvate decarboxylase, pyruvate decarboxylase, the acetyl phosphate-producing pyruvate oxidase, and the acetate-producing pyruvate oxidase (42) (sequence identities between *B. fragilis* Ppyr decarboxylase and these proteins with a sequence range of 23–29%). The chemical reactions catalyzed by these enzymes are shown in Fig. 5. The common chemistry catalyzed by the family of enzymes is the decarboxylation of an α-keto carboxylate using the TPP cofactor as an "electron sink."

Metal Ion and TPP Activation—Metal-free Ppyr decarboxylase, prepared by exhaustive dialysis, is inactive. The metal ions Mg(II), Mn(II), Ca(II), Co(II), Ni(II), and Zn(II) were tested (at a concentration of 1 or 5 mM) as activators of the metal-free enzyme in the presence of 1.5 mM TPP and saturating Ppyr (50 μM). Only Mg(II), Mn(II), and Ca(II) were activators. The k_{cat} and K_m values (corresponding to the K_d for metal ion dissociation from the enzyme-TPP-Ppyr-M(II) complex) are listed in Table II. Whereas the k_{cat} values of the Mg(II)-, Mn(II)-, and

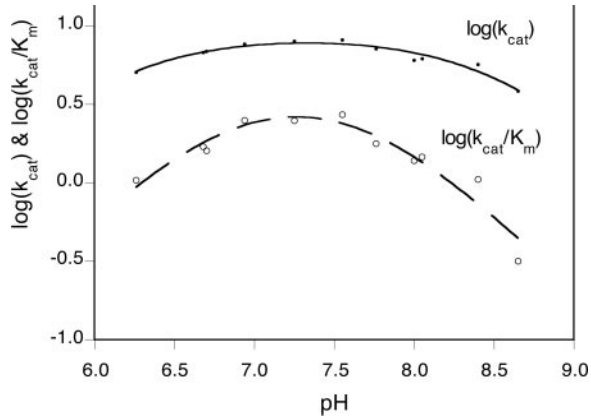

FIG. 7. **pH rate profiles of Ppyr decarboxylase catalysis.** See "Experimental Procedures" for details. The apparent pK_a of 6.1 ± 0.1 and pK_a of 8.5 ± 0.1 were obtained by computer fitting the log k_{cat} profile to Equation 2, and pK_a of 6.7 ± 0.2 and pK_a of 7.7 ± 0.2 were obtained by computer fitting the log (k_{cat}/K_m) profile.

Ca(II)-activated decarboxylase are similar (~10 s^{-1}), the K_m for Mn(II) (13 μM) is significantly smaller than the K_m values of Mg(II) and Ca(II) (~80 μM).

TPP-free Ppyr decarboxylase, also prepared by exhaustive dialysis, is inactive. The K_m for TPP activation was determined by measuring the initial velocity of the Mg(II) (5 mM)/Mn(II) (1 mM)-activated Ppyr decarboxylase-catalyzed decarboxylation of Ppyr (saturating at 50 μM). The initial velocity data defined the k_{cat} = 9.7 ± 0.3 s^{-1} and TPP K_m = 13 ± 2 μM. Other TPP-activated enzymes are known to bind TPP with K_d values in the nanomolar to micromolar range (43, 44).

Mg(II) and TPP-binding Residues—The results described above show that Ppyr decarboxylase, like the other α-keto decarboxylases of this enzyme family, requires TPP and Mg(II) as cofactors. Based on the known three-dimensional structures of several of these family members (41, 45–50), it has been shown that the Mg(II) cofactor functions to anchor the TPP by coordinating to two of the phosphate oxygen atoms and to the side chains of an active site Asp and Asn. The Asp and Asn residues are located at opposite ends of the TPP-binding sequence motif (51) illustrated in Fig. 6. In Ppyr decarboxylase, the Asp residue is Asp-260. The site-directed mutant D260A was prepared to test the contribution of Asp-260 to catalysis. The steady-state kinetic constants of this mutant were determined to be $k_{cat} = 0.01\ s^{-1}$, $K_m = 17\ \mu M$, and $k_{cat}/K_m = 6 \times 10^2\ s^{-1}\ M^{-1}$. Whereas the K_m is increased only 5-fold, the catalytic turnover rate of the mutant enzyme is 1000-fold lower than that of the wild-type enzyme (Table II). Thus, Asp-260 is an important contributor to catalysis. This result is consistent with the assignment of the TPP-binding sequence motif in Ppyr decarboxylase as indicated in Fig. 6.

The N1′(H) of the pyridinium ring is bound through a H-bond to a Glu side chain located near the N terminus. The Ppyr decarboxylase and sulfopyruvate decarboxylase (<400 amino acids) are both considerably smaller than the TPP-binding subunits of acetolactate synthase, benzoylformate decarboxylase, and pyruvate oxidase/dehydrogenase (~600 amino acids). Nevertheless, the ClustalW sequence alignment (see Fig. 6) identifies this Glu as stringently conserved within the enzyme superfamily, including the Ppyr decarboxylase and sulfopyruvate decarboxylase subfamilies. In the *B. fragilis* Ppyr decarboxylase this TPP-binding residue is Glu-49.

Mutagenesis Probe of Carboxylate Residues Unique to the Sulfopyruvate and Ppyr Decarboxylases—Aside from total charge (−1 and −2, respectively) of the anionic C (3) substituent, the structures of sulfopyruvate and phosphonopyruvate are quite similar. In this study, sulfopyruvate was shown to be a competitive inhibitor of Ppyr decarboxylase (at pH 7, 25 °C) with a $K_i = 200 \pm 20\ \mu M$. Furthermore, ^1H NMR analysis of a reaction mixture initially containing 0.5 μM Ppyr decarboxylase, 1 mM sulfopyruvate, 1 mM $MgCl_2$, and 0.4 mM TPP in 10 mM K^+HEPES (pH 7.6, 25 °C) revealed that 15% of the sulfopyruvate had been converted to sulfoacetaldehyde (identified by the aldehyde proton signal at 9.3 parts/million) within the 1.5-h incubation period. Because sulfopyruvate is a competitive inhibitor of, and a substrate ($k_{cat} \sim 0.05\ s^{-1}$) for, the Ppyr decarboxylase, it is reasonable to anticipate that the active sites of the sulfopyruvate decarboxylase and Ppyr decarboxylases share common features that extend beyond the TPP cofactor and Mg(II)-binding sites. Indeed, stringently conserved polar residues of Ppyr decarboxylase, which are found in the sulfopyruvate decarboxylase sequences, total 16 in number. Subtracting the polar residues conserved among all family members, there are 12 residues that are common only to the sulfopyruvate and Ppyr decarboxylases. One residue, in particular, was the Asp-258 that flanks the TTP-binding sequence motif "G259D260 . . . " in Ppyr decarboxylase. The site-directed mutant D258A was prepared to access the degree to which Asp-258 contributes to catalysis in Ppyr decarboxylase. The steady-state kinetic constants of this mutant were determined to be $k_{cat} = 1\ s^{-1}$, $K_m = 2.1$ mM and $k_{cat}/K_m = 5 \times 10^2\ s^{-1}\ M^{-1}$. Whereas the catalytic turnover rate in this mutant is only 10-fold less than that of the wild-type enzyme, the K_m is increased ~1000-fold (Table III). Thus, Asp-258 is especially important to substrate binding.

A second polar residue uniquely common to the sulfopyruvate and Ppyr decarboxylases was Glu-213 (identified in Fig. 6), for which the E213A mutant was prepared. The kinetic constants obtained for the E213A mutant ($k_{cat} = 0.5\ s^{-1}$, $K_m = 2.6\ \mu M$, and $k_{cat}/K_m = 2 \times 10^5\ s^{-1}\ M^{-1}$) indicated only a 20-fold reduction in activity. In contrast to Asp-258 and Asp-260, Glu-213 does not appear to play an important role in Ppyr decarboxylase catalysis.

The Importance of the Phosphonopyruvate "Phosphono" Group in Ppyr Decarboxylase Substrate Recognition—Pyruvate was shown to be a slow substrate with the kinetic constants $k_{cat} = 0.05\ s^{-1}$, $K_m = 25$ mM, and $k_{cat}/K_m = 2\ s^{-1}\ M^{-1}$. A comparison of these values with those obtained with phosphonopyruvate (Table III) reveals the importance of the pyruvate C (3)-PO_3^{-2} group in substrate activity. Using pyruvate as the substrate for the Ppyr decarboxylase, Pald was shown to be a competitive inhibitor with a $K_i = 15 \pm 2\ \mu M$. The large difference in the values of the phosphonopyruvate and pyruvate K_m constants (3 μM *versus* 25 mM) and in values of the Pald (−2 charge on the phosphono group) and sulfopyruvate (−1 charge on the sulfo group) K_i constants (15 *versus* 200 μM), shows that the phosphonopyruvate "phosphono" group, and not the carboxyl group, is the major source of enzyme-substrate binding energy.

pH Dependence of Catalysis—The pH rate profile analysis defined pH 7.0–7.5 as the pH range for optimal Ppyr decarboxylase catalysis. Both the log k_{cat} and log (k_{cat}/K_m) pH profiles were bell-shaped (Fig. 7). Computer fitting of the log k_{cat} profile gave an apparent pK_a of 6.1 ± 0.1 for the essential base within the enzyme-substrate complex, and an apparent pK_a of 8.5 ± 0.1 for the essential acid within the enzyme-substrate complex. Computer fitting of the log (k_{cat}/K_m) profile gave an apparent pK_a of 6.7 ± 0.2 for the essential base within the uncomplexed substrate or enzyme and an apparent pK_a of 7.7 ± 0.2 for the essential acid within the uncomplexed substrate or enzyme.

Conclusion—The identity of the resultant product of the *aepY* gene in the *B. fragilis* genome has been shown to be Ppyr decarboxylase. This enzyme is a trimer of a 41,184-Da subunit, which shares sequence homology (global and cofactor-binding sequence motifs) with members of a superfamily of TPP- and Mg(II)-dependent α-ketodecarboxylases that includes sulfopyruvate decarboxylase, pyruvate decarboxylase and oxidase, acetolactate synthase, and benzoylformate decarboxylase. The phosphonopyruvate C(3)-PO_3^{2-} group plays an important role in Ppyr decarboxylase binding. Nevertheless, sulfopyruvate and pyruvate are slow substrates for the Ppyr decarboxylase, indicative of lax substrate specificity.

REFERENCES

1. Baumann, H., Tzianabos, A. O., Brisson, J. R., Kasper, D. L., and Jennings, H. J. (1992) *Biochemistry* **31,** 4081–4089
2. Tzianabos, A. O., Chandraker, A., Kalka-Moll, W., Stingele, F., Dong, V. M., Finberg, R. W., Peach, R., and Sayegh, M. H. (2000) *Infect. Immun.* **68,** 6650–6655
3. Tzianabos, A. O., Pantosti, A., Baumann, H., Brisson, J. R., Jennings, H. J., and Kasper, D. L. (1992) *J. Biol. Chem.* **267,** 18230–18235
4. Tzianabos, A. O., Onderdonk, A. B., Rosner, B., Cisneros, R. L., and Kasper, D. L. (1993) *Science* **262,** 416–419
5. Kalka-Moll, W. M., Wang, Y., Comstock, L. E., Gonzalez, S. E., Tzianabos, A. O., and Kasper, D. L. (2001) *Infect. Immun.* **69,** 2339–2344
6. Wang, Y., Kalka-Moll, W. M., Roehrl, M. H., and Kasper, D. L. (2000) *Proc. Natl. Acad. Sci. U. S. A.* **97,** 13478–13483
7. Heise, N., Raper, J., Buxbaum, L. U., Peranovich, T. M., and de Almeida, M. L. (1996) *J. Biol. Chem.* **271,** 16877–16887
8. Shin, J. E., Ackloo, S., Mainkar, A. S., Monteiro, M. A., Pang, H., Penner, J. L., and Aspinall, G. O. (1997) *Carbohydr. Res.* **305,** 223–232
9. Kennedy, K. E., and Thompson, G. A., Jr. (1970) *Science* **168,** 989–991
10. Steiner, S., Conti, S. F., and Lester, R. L. (1973) *J. Bacteriol.* **116,** 1199–1211
11. Wassef, M. K., and Hendrix, J. W. (1976) *Biochim. Biophys. Acta* **486,** 172–178
12. Serrano, A. A., Schenkman, S., Yoshida, N., Mehlert, A., Richardson, J. M., and Ferguson, M. A. (1995) *J. Biol. Chem.* **270,** 27244–27253
13. Coyne, M. J., Kalka-Moll, W., Tzianabos, A. O., Kasper, D. L., and Comstock, L. E. (2000) *Infect. Immun.* **68,** 6176–6181
14. Barry, R. J., Bowman, E., McQueney, M., and Dunaway-Mariano, D. (1988) *Biochem. Biophys. Res. Commun.* **153,** 177–182
15. Liang, C. R., and Rosenberg, H. (1968) *Biochim. Biophys. Acta* **156,** 437–439

16. Warren, W. A. (1968) *Biochim. Biophys. Acta* **156,** 340–346
17. Deleted in proof
18. Kim, A., Kim, J., Martin, B. M., and Dunaway-Mariano, D. (1998) *J. Biol. Chem.* **273,** 4443–4448
19. Jia, Y., Lu, Z., Huang, K., Herzberg, O., and Dunaway-Mariano, D. (1999) *Biochemistry* **38,** 14165–14173
20. Liu, S., Lu, Z., Jia, Y., Dunaway-Mariano, D., and Herzberg, O. (2002) *Biochemistry* **41,** 10270–10276
21. Kim, J. B. (1994) *Investigations of 2-Aminoethylphosphonate Biosynthetic Enzymes in Tetrahymena Pyriformis.* Ph.D. thesis, University of Maryland, College Park, MD
22. Nakashita, H., Kozuka, K., Hidaka, T., Hara, O., and Seto, H. (2000) *Biochim. Biophys. Acta* **1490,** 159–162
23. Thompson, C. J., and Seto, H. (1995) *Biotechnology* **28,** 197–222
24. Seto, H., and Kuzuyama, T. (1999) *Nat. Prod. Rep.* **16,** 589–596
25. Schwartz, D., Recktenwald, J., Pelzer, S., and Wohlleben, W. (1998) *FEMS Microbiol. Lett.* **163,** 149–157
26. Nakashita, H., Watanabe, K., Hara, O., Hidaka, T., and Seto, H. (1997) *J. Antibiot.* (*Tokyo*) **50,** 212–219
27. Cassaigne, A., Lacoste, A. M., and Neuzil, E. (1976) *C. R. Hebd. Seances Acad. Sci. Ser. D Sci. Nat.* **282,** 1637–1639
28. Jiang, W., Metcalf, W. W., Lee, K. S., and Wanner, B. L. (1995) *J. Bacteriol.* **177,** 6411–6421
29. Parker, G. F., Higgins, T. P., Hawkes, T., and Robson, R. L. (1999) *J. Bacteriol.* **181,** 389–395
30. Ternan, N. G., and Quinn, J. P. (1998) *Syst. Appl. Microbiol.* **21,** 346–352
31. La Nauze, J. M., Rosenberg, H., and Shaw, D. C. (1970) *Biochim. Biophys. Acta* **212,** 332–350
32. Kim, A. D., Baker, A. S., Dunaway-Mariano, D., Metcalf, W. W., Wanner, B. L., and Martin, B. M. (2002) *J. Bacteriol.* **184,** 4134–4140
33. Anderson, V. E., Weiss, P. M., and Cleland, W. W. (1984) *Biochemistry* **23,** 2779–2786
34. White, R. H. (1986) *Biochemistry* **25,** 5304–5308
35. Baker, A. S., Ciocci, M. J., Metcalf, W. W., Kim, J., Babbitt, P. C., Wanner, B. L., Martin, B. M., and Dunaway-Mariano, D. (1998) *Biochemistry* **37,** 9305–9315
36. Appel, R. D., Bairoch, A., and Hochstrasser, D. F. (1994) *Trends Biochem. Sci.* **19,** 258–260
37. Bradford, M. M. (1976) *Anal. Biochem.* **72,** 248–254
38. DiMarco, A. A., Bobik, T. A., and Wolfe, R. S. (1990) *Annu. Rev. Biochem.* **59,** 355–394
39. Graupner, M., Xu, H., and White, R. H. (2000) *J. Bacteriol.* **182,** 4862–4867
40. Chipman, D., Barak, Z., and Schloss, J. V. (1998) *Biochim. Biophys. Acta* **1385,** 401–419
41. Hasson, M. S., Muscate, A., McLeish, M. J., Polovnikova, L. S., Gerlt, J. A., Kenyon, G. L., Petsko, G. A., and Ringe, D. (1998) *Biochemistry* **37,** 9918–9930
42. Schellenberger, A. (1998) *Biochim. Biophys. Acta* **1385,** 177–186
43. Tate, J. R., and Nixon, P. F. (1987) *Anal. Biochem.* **160,** 78–87
44. Jung, E. H., Takeuchi, T., Nishino, K., and Itokawa, Y. (1988) *Int. J. Biochem.* **20,** 1255–1259
45. Muller, Y. A., Lindqvist, Y., Furey, W., Schulz, G. E., Jordan, F., and Schneider, G. (1993) *Structure* **1,** 95–103
46. Muller, Y. A., and Schulz, G. E. (1993) *Science* **259,** 965–967
47. Dyda, F., Furey, W., Swaminathan, S., Sax, M., Farrenkopf, B., and Jordan, F. (1993) *Biochemistry* **32,** 6165–6170
48. Arjunan, P., Umland, T., Dyda, F., Swaminathan, S., Furey, W., Sax, M., Farrenkopf, B., Gao, Y., Zhang, D., and Jordan, F. (1996) *J. Mol. Biol.* **256,** 590–600
49. Dobritzsch, D., Konig, S., Schneider, G., and Lu, G. (1998) *J. Biol. Chem.* **273,** 20196–20204
50. Pang, S. S., Duggleby, R. G., and Guddat, L. W. (2002) *J. Mol. Biol.* **317,** 249–262
51. Hawkins, C. F., Borges, A., and Perham, R. N. (1989) *FEBS Lett.* **255,** 77–82